Acta Cryst. (1998). A**54**, 91–101

MSLS, a Least-Squares Procedure for Accurate Crystal Structure Refinement from Dynamical Electron Diffraction Patterns

J. JANSEN,[a,b]* D. TANG,[a] H. W. ZANDBERGEN[a] AND H. SCHENK[b]

[a]*National Centre for HREM, Laboratory of Materials Science, Delft University of Technology, Rotterdamseweg 137, 2628 AL Delft, The Netherlands, and* [b]*Laboratory of Crystallography, University of Amsterdam, Nieuwe Achtergracht 166, 1018 WV Amsterdam, The Netherlands. E-mail: joukj@crys.chem.uva.nl*

(*Received 26 August 1996; accepted 11 August 1997*)

Abstract

In X-ray crystallography, a least-squares structure refinement is used to two purposes: to prove the correctness of the proposed model and to improve it. In electron crystallography, the same tool would be desirable. However, the standard programs for least-squares structure refinement used in X-ray diffraction may give wrong results using electron diffraction data because the kinematically calculated diffracted intensity is not valid for the interaction of electrons and crystals thicker than about 20 Å for strong scatterers. In this paper, a new approach is presented that overcomes this problem and in addition takes into account all the advantages contained in dynamic scattering. The multislice method, well known in high-resolution electron microscopy (HREM), was combined with a least-squares algorithm, resulting in the multislice least-squares (*MSLS*) procedure. Experiments show that the atomic positions obtained by the new procedure are of the same accuracy as those obtained from single-crystal X-ray diffraction. However, the size of the single crystals used is much smaller (diameters down to ±100 Å). Also, light-atom positions can be determined with high precision by using data sets from crystal areas with different thicknesses. The multislice refinement gave good results up to 150 to 400 Å depending on the composition of the crystal, with R values based on the intensities of less than 5%. An additional advantage of the approach is that some extra quantities (*e.g.* crystal thickness, crystal orientation) can be refined at the same time.

1. Introduction

At present, several advanced types of high-resolution electron microscopes operating at intermediate accelerating voltages (200–400 keV) have a point-to-point resolution of about 1.8 Å. For very thin specimens and at Scherzer focus, one can interpret dots down to this distance directly as atom columns. Information with spatial frequencies beyond this point-to-point resolution can exist in the images but this information is delocalized. In principle, the information extends to a limit, called the information limit of the microscope, which is about 1.1 Å for microscopes with a field-emission gun. The point-to-point resolution is governed by the spherical aberration of the objective lens, while the information limit is determined by a damping envelope, which depends on the energy spread of the primary electrons and the instability of the current of the objective lens. The typical approaches to extend the interpretable information down to the information limit of the microscope are:

(i) The conventional method of extensive image calculations in which one calculates the images for a given model using the partly known microscope parameters and comparing these with experimental images.

(ii) The use of a much higher accelerating voltage (about 1 MeV) with a high-quality objective lens. In this case, the resolution of the images is only limited by the damping envelope of the microscope, since the theoretical point-to-point resolution is close to or even beyond the information limit.

(iii) Exit wave reconstruction methods initiated by Kirkland (1980) and developed by Van Dyck & Op De Beeck (1992) (through-focus method), Lichte (1991) (off-axis holography) and Kirkland, Saxton, Chau, Tsuno & Kawasaki (1995) (tilted-beam series), which allow direct interpretation up to the information limit of the electron microscope and possibly even beyond that (Kirkland *et al.*, 1995).

The information in diffraction space proceeds much further (*e.g.* 0.8 Å is rather easy to achieve). This is because, in contrast with the image in real space, the diffraction information is not restricted by the aberrations of the objective lens or the chromatic aberrations. This also implies that the information at about 0.8 Å can be collected by relatively cheap electron microscopes in diffraction mode. To acquire accurate integrated intensities, small diffraction spots coming from an illuminated area of uniform thickness is essential. A field-emission gun is ideal to achieve a small probe size, high brightness and an almost parallel beam.

The drawback of diffraction information is that only the diffracted intensity can be recorded and not its phase. Thus, a structure cannot be determined from the intensities directly. The phases have to be measured or

estimated in some way. For X-ray diffraction by crystalline material, several procedures such as direct methods and the Patterson method are available to solve this phase problem, which is typical for all diffraction experiments.

Recently, some successful methods for *ab initio* crystal structure determination from electron diffraction data were reported. Dorset, Kopp, Fryer & Tivol (1995) use the Sayres equation to expand an initial phase set. With convergent-beam diffraction patterns, phases can be determined experimentally from overlapping discs (Midgley, Saunders, Vincent & Steeds, 1995; Zuo, Høier & Spence, 1989).

Another approach, not using diffraction data, is taken by the program *CRISP* (Hovmöler, 1992), which uses the phases determined from Fourier transforms of the corresponding HREM images. The images are sharpened by modifying the phase set to crystallographic allowed phases (*e.g.* 0 and π for centrosymmetric space groups).

Such *ab initio* methods only give a rough model of a possible structure, mostly because only some of the phases are correctly determined. The correctness of the resulting structural model has to be proven by comparing it with the measured data by, for example, a least-squares-refinement procedure, which is of common use in X-ray diffraction.

However, the standard refinement programs, developed for X-ray diffraction, cannot be applied directly in the case of electron diffraction for two reasons:

(i) Most of the reflections in a pattern along a zone axis are not exact in Bragg position. Thus, for each measured reflection, a correction is needed, which depends not only on the distance of the reflection to the Ewald sphere but also on the crystal thickness.

(ii) Since the interaction of electrons with matter is strong, multiple scattering is a normal phenomenon for electrons. Therefore, the kinematical diffraction theory, which is a good approximation in X-ray crystallography, is no longer valid for electrons and the dynamical diffraction theory should be used.

As far as we know, three approaches have been reported previously in which dynamical diffraction was taken into account in the refinement process.

(i) Zuo & Spence (1991) used convergent-beam electron diffraction (CBED) to refine structure factors. From these structure factors, structural parameters were deduced. Vincent & Exelby (1995) use HOLZ and CBED to refine some structural parameters. These methods are limited to small unit cells owing to the effect that computing time increases exponentially with the number of variables to be refined and with the complexity of the convergent-beam patterns.

(ii) Tsuda & Tanaka (1995) were able to refine a small number of parameters for $SrTiO_3$ using convergent-beam patterns. It proved to work for rather thick crystals (in their example ~200 Å). This large thickness value is needed since it is essential to be able to estimate the actual thickness with convergent-beam techniques. The usefulness of this method is limited because of the huge calculation time. Since many CBED patterns have to be calculated, only a very limited number of parameters can be taken into account. More parameters will increase the computing time exponentially. At present, Debye–Waller factors of the three independent atoms were reported to be refined.

(iii) Sha, Fan & Li (1993) proposed a different approach using *normal* diffraction patterns recorded with a more or less parallel illumination. They developed a method to correct the intensities obtained from this pattern for the dynamical effect using the knowledge of a rough atomic model. The method uses a multislice calculation to determine thickness. It is assumed that the same relation between kinematic structure factor and dynamic structure factor holds. In this way, a quasi-kinematical data set can be calculated, which can subsequently be used in a standard kinematical refinement procedure. By this method, better models can be found. A drawback is that the two procedures are used separately and that a wrong initial model may affect the results of the refinement.

In this paper, we report a least-squares procedure that fully takes into account the dynamical diffraction within the refinement procedure. The advantage of this treatment is that, apart from the parameters related to the crystal structure, parameters such as crystal thickness, crystal orientation and absorption factor can be refined simultaneously. In fact, our method will be rather complementary to the CBED methods. Our method aims at thinner crystals and due to a faster calculation it can handle more parameters at the same time.

2. Multislice least squares, the program *MSLS*

We have developed a computer program, *MSLS*, to incorporate the dynamical diffraction theory into the structure-refinement process. The program combines two known algorithms: the multislice method (Cowley & Moodie, 1957) and a least-squares-fitting procedure.

The multislice calculations in *MSLS* are based on our own computer program This procedure was tested very thoroughly. Comparison with other simulation programs yields the same results as many algorithms (Op De Beeck, 1996, 1997). The calculation takes into account both the curvature of the Ewald sphere and multiple scattering. Since the calculations are rather lengthy, we made some simplifications and approximations. High-order Laue-zone (HOLZ) lines were not included in the calculations. The program uses equal subslices of arbitrary size. A stable result can be achieved if the slice thickness is at most 1 Å, depending on the scatterers in the crystal. By taking equal subslices, one assumes that the actual positions of the atoms along the zone axis can be approximated by an average scattering density along this axis. This is the same assumption as is made in the Van Dyck (1993) column approach. This column

approximation implies that the slice size is arbitrary. However, during calculation the cell dimension in the beam direction was an integer multiple of the slice size, except for the last slice. The reason for this last slice will be discussed later in this article.

The least-squares algorithm is basically the linearized nonlinear algorithm that is in common use in crystallographic structure refinement (Giacovazzo *et al.*, 1992). It tries to minimize an R factor defined by

$$R = \sum\{I_m^{\rm obs} - I_m\}^2 / \sum\{I_m^{\rm obs}\}^2. \quad (1)$$

The main part of the algorithm is a set of linear equations for parameter shifts **s**:

$$\mathbf{Ms} = \mathbf{v}, \quad (2)$$

where the refinement matrix is given by

$$M_{ij} = \sum_m w_m(\partial I_m/\partial p_j)(\partial I_m/\partial p_i) \quad (3)$$

and the vector by

$$v_i = \sum_m w_m(I_m - I_m^{\rm obs})(\partial I_m/\partial p_i). \quad (4)$$

$I_m^{\rm obs}$ are the observed reflection intensities and I_m are the calculated reflection intensities; p_i is the ith parameter to be refined and w_m are the weights of the reflections. In theory, these weights should be $1/\sigma(I)^2$, in which $\sigma(I)$ is the standard deviation of the intensity. Unless the intensities depend linearly on the parameters, the process should be iterated until convergence is reached.

The derivative of the intensity I_m with respect to the parameters p_i raises some problems. The multislice algorithm is an iterative process for which no analytical function is available. So the derivatives cannot be calculated analytically. In *MSLS*, these derivatives are numerically calculated using the definition of the derivative

$$I'(p) = [I(p + \delta) - I(p)]/\delta \quad (5)$$

with δ tending to zero. Numerically, one can only take a finite value for δ. However, δ cannot be too small, owing to the accuracy of the computer. A too small δ will cause a random difference between $I(p + \delta)$ and $I(p)$ of the order of the numerical accuracy of the computer. In practice, this difference will tend to zero and leads to a singular least-squares matrix **M**. In the next section, the best values of δ will be discussed.

Just as in a traditional structure-refinement program, the parameters in *MSLS* include atomic positions, Debye–Waller factors, scaling factors *etc.* At the moment, only isotropic Debye–Waller factors are used Anisotropic temperature factors will increase the number of parameters in the least-squares procedure. In that case, the ratio of the number of parameters to the number of observed reflections will become worse. To get more intensities (from other zones) is limited due to experimental reasons: at present, all zones have to be selected and oriented by hand and sometimes it is hard to prepare samples to get the right orientations of the crystals. As a result of using the multislice method, some more parameters may be involved: the crystal thickness, the crystal misalignment and absorption parameters. The misalignment of the crystal is expressed in terms of the centre of the Laue circle in the pattern. A crystal tilt results in a corresponding shift of this centre. Note that crystal tilt and beam tilt are equivalent for diffraction patterns. Therefore, we do not consider beam tilt in this paper.

The refinement of the thickness requires a special trick. The derivatives, I' [formula (5)], imply that the dependency of the intensity on the thickness is continuous. However, division of the crystal in as many slices as in the multislice calculation gives the thickness as a discrete parameter. If δ in (5) is smaller than the slice size, the resulting derivative will be zero in many cases since $I(p + \delta)$ and $I(p)$ are equal owing to the calculation method. To overcome this problem, in *MSLS* a crystal is divided in a certain number of equal slices and a last slice having a thickness of a fraction f of the other slices. It is assumed that this slice contains the same scattering potential as that of the other slices but multiplied by f.

Diffraction patterns may always be multiplied by a constant factor without changing the physics of the system. In *MSLS*, this is a scaling factor that is needed to scale the observed and calculated intensities to the same order of magnitude. This scaling factor is one of the refinable parameters. However, one has to take care with the definition of this factor. It should be defined in such a way that it is not dependent on the change of any other parameter in the refinement procedure, in particular the crystal thickness and the absorption parameter. Therefore, the actual scaling factor, S, was expressed as a function of s, the parameter that was used in the refinement process:

$$S = s \sum_{\mathbf{H}\neq\mathbf{0}} I_{\mathbf{H}}^{\rm obs} \Big/ \sum_{\mathbf{H}\neq\mathbf{0}} I_{\mathbf{H}}^{\rm calc}. \quad (6)$$

This results in the ideal case in a scaling factor s of 1.0.

In order to get three-dimensional crystal structure data from an electron diffraction pattern, one zone is not enough in general, though for high-symmetry space groups one special zone may be sufficient. *MSLS* allows for simultaneous refinement of several diffraction patterns, each with its own parameters for scaling, thickness and crystal alignment.

3. Testing and optimizing the procedure

The newly developed method was firstly tested on simulated electron diffraction data, which allowed complete control of the whole process. Since *MSLS* is based on calculating intensities, we have chosen a simulation method that is different from the multislice

Table 1. *Atomic model of LuNiBC used for simulations*

Space group: *P4/nmm*. $a = 3.49850$, $b = 3.49850$, $c = 7.75560$ Å, $\alpha = 90$, $\beta = 90$, $\gamma = 90°$.

	x	y	z	B (Å^2)
Lu	1/4	1/4	0.16	2.5
Ni	3/4	1/4	1/2	2.5
C	3/4	3/4	0.15	4.0
B	3/4	3/4	0.35	4.0

Table 2. *Atomic model of CPCN used for simulations*

Space group: *Pnma*. $a = 7.244$, $b = 7.821$, $c = 6.916$ Å, $\alpha = 90$, $\beta = 90$, $\gamma = 90°$.

	x	y	z	B (Å^2)
C1	0.1727	0.1556	0.8665	3.98
C2	0.0361	1/4	0.9919	3.41
C3	0.0609	1/4	0.1976	3.43
N	0.0787	1/4	0.3617	4.37
H1	0.274	0.099	0.933	4.9
H2	0.123	0.098	0.752	5.6
H3	0.909	1/4	0.955	5.6

algorithm in *MSLS*. The Bloch-wave method of the *EMS* package (Stadelmann, 1987) was selected for this purpose.

Several structures containing equal atoms or containing mixtures of heavy and light atoms were used, including *e.g.* LuNiBC (Table 1) and CPCN (Table 2). Thicknesses up to 120 Å were tested. Misalignment of the crystal was limited to a few milliradians, which is common in experiments.

All parameters refined to their true values within the margins expected due to numerical errors, except when thickness and Debye–Waller factors were refined simultaneously. The correlation between thickness and Debye–Waller factors is addressed in detail in the *Discussion*. Each parameter needs a good guess as starting value. How close the parameter has to be to the *true* value depends on the problem. In our experience, for instance, the crystal thickness may have a starting value about 50 Å off the *true* value.

The simulated data were also used to determine experimentally the best values of δ to calculate the derivatives with formula (5). As expected, the best value for δ was a fraction of the associated parameter, p. A threshold for too small values had to be imposed to avoid problems caused by the limited accuracy of computers. It appeared that the same fraction and threshold could be used for all parameters except for crystal thickness. The best convergence was achieved when

$$\delta = \max(p \times 10^{-5}, 0.01) \tag{7}$$

for all parameters except the crystal thickness. For the crystal thickness, this parameter was optimized to be

$$\delta = \max(p \times 10^{-7}, 0.0001). \tag{8}$$

4. Experimental results

The multislice least-squares procedure was tested on real experimental data for several compounds. Three crystal structures will be discussed in this paper. The results will be compared with those of either single-crystal X-ray diffraction or Rietveld refinements on neutron powder diffraction data. They will also be compared with kinematical refinements on the same electron diffraction data.

To obtain thin enough areas, the samples were crushed. Electron diffraction patterns were taken with a Philips CM30ST electron microscope equipped with a field-emission gun and operated at 300 keV. A typical spot size of 100 Å was used to illuminate the thinner areas close to the edges of the crystals. The diffraction patterns were recorded using a Tietz software package and a 1024 × 1024 pixel Photometric CCD camera having a dynamic range of 12 bits. All data files were corrected for gain variations using a standard flatfielding procedure. The oversaturated areas of the CCD were not taken into account. Although *MSLS* can compensate for the misalignment of the crystal by locating the centre of the Laue circle, for initial tests we would like the crystal to be orientated along a zone axis as perfectly as possible. In diffraction space, this appears as a symmetric pattern (*e.g.* $I_{\mathbf{H}} = I_{-\mathbf{H}}$ for a centrosymmetric crystal). Diffraction patterns that were close to this symmetry were selected for further processing (see for instance Fig. 1). So, only a small misalignment correction is needed, which can be determined within the refinement process starting from the assumption that the crystal is perfectly aligned.

The integrated intensity of each reflection was determined by enclosing the reflection spot by a rectangle, of which the edges were used to estimate the background (a new version of the program will also handle circular boxes). The number of pixels inside the boxes is typically between 20 and 300. By correcting with the background from the edge of the box, one assumes that the background under the peak behaves linearly. The background should be removed since it contains information one is not interested in, *i.e.* from inelastic scattering or amorphous layers. These indexed intensities were then employed as input for *MSLS*.

Three example structures, $La_3Ni_2B_2N_3$ (Zandbergen, Jansen, Cava, Krajewski & Peck, 1994), $ThPd_{0.65}B_{4.7}$ (Zandbergen *et al.*, 1995) and $Ce_5Cu_{19}P_{12}$ (Cava *et al.*, 1997) were tested. All of them were also refined using a standard kinematical program for comparison. The refinement with *MSLS* was based on exactly the same data sets as used for the kinematical refinement. In the case of the kinematical refinement, the crystal thickness should be estimated since a correction for the curvature of the Ewald sphere should be applied. With trial and error for several thicknesses, the best thickness was assumed to be the one giving the best R value in the refinement.

Table 3. *The structure model of $La_3Ni_2B_2N_3$*

Space group: $I4/mmm$. $a = 3.73$, $b = 3.73$, $c = 20.67$ Å, $\alpha = 90$, $\beta = 90$, $\gamma = 90°$.

	x	y	z
La1	0	0	0
La2	1/2	1/2	z
Ni	1/2	0	1/4
B	0	0	z
N1	1/2	1/2	0
N2	0	0	z

4.1. *$La_3Ni_2B_2N_3$*

For $La_3Ni_2B_2N_3$, diffraction patterns in the [100] and [110] directions were recorded. A kinematical refinement using these electron diffraction data was reported previously (Zandbergen *et al.*, 1994). A Rietveld refinement on neutron diffraction data from the same structure was also performed (Huang *et al.*, 1995). Table 3 shows the general structure of $La_3Ni_2B_2N_3$ and Table 4 is a comparison of the refined z coordinates of the two published methods and those obtained with *MSLS*. Additional refinement data can be found in Table 5. Since the neutron diffraction method is an accepted method, we assume the structure determined by this method to be the correct one. It is evident that *MSLS* gives within the accuracy of the data exactly the same results, whereas the kinematic refinement shows a slight error. The crystal thicknesses found by *MSLS* were 48 (10) Å for the [100] zone and 78 (11) Å for the [110] zone. These values are quite different from the 30 Å assumed in the kinematical refinement (Zandbergen *et*

Table 4. *Comparison of the z coordinates of $La_3Ni_2B_2N_3$ refined using either Rietveld methods on neutron data or kinenematic or dynamic refinement on electron diffraction data*

	Neutron	Kinematic	*MSLS*
La2	0.1295 (1)	0.128 (1)	0.127 (2)
B	0.1946 (2)	0.221 (3)	0.196 (2)
N2	0.1246 (1)	0.135 (5)	0.117 (3)

Table 5. *Refinement results for $La_3Ni_2B_2N_3$ using MSLS*

The number of reflections given are observed intensities $I > 2\sigma(I)$ which were used in the R-factor calculation.

	Overall	(100)	(110)
R (%)	4.1	1.0	8.3
Thickness (Å)		48 (10)	78 (11)
h-Laue circle		0.0	0.17 (18)
k-Laue circle		−1.5 (4)	−0.17 (18)
l-Laue circle		−10 (3)	−0.6 (14)
No. of reflections	311	185	126
Absorption	0.00003 (3)		

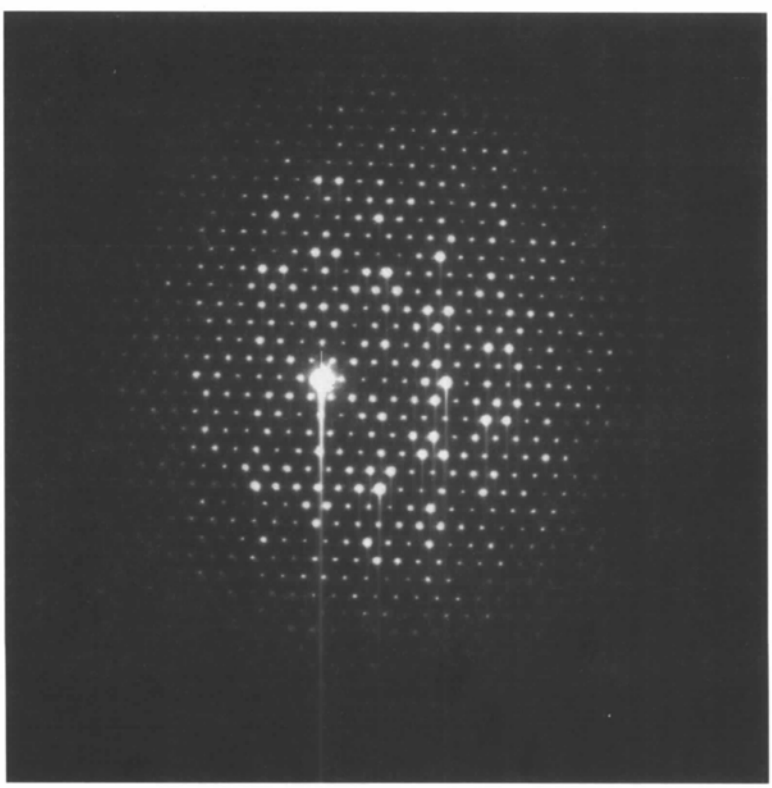

Fig. 1. Diffraction pattern of $Ce_5Cu_{19}P_{12}$ in the [001] direction.

al., 1994). Fig. 2 shows the intensity as a function of thickness for some arbitrary reflections. In the case of the kinematic approximation, a linear function is to be expected. From Fig. 2, it is clear that the kinematic theory is not valid any more.

4.2. $ThPd_xB_{6-2x}$

A partial successful kinematical refinement of $ThPd_{0.65}B_{4.7}$ has been reported (Zandbergen *et al.*, 1995), in which only the heavier atoms Th and Pd could be found. The position of the B atom could not be determined, although several diffraction patterns, [100], [110], [111] and [120], were incorporated in the refinement procedure. Another problem of this structure is that the Pd and B positions are not fully occupied. From element analysis [electron probe microanalysis (EPMA)], it was found (Zandbergen *et al.*, 1995) that in this phase the ratio of Th, Pd and B is about 1:0.65:4.7. The model proposed is a mixture of a ThB_6 and a $ThPd_3$ structure where B atoms are close to the Pd vacancies and *vice versa*. This is logical from a structural chemistry point of view since the occupied Pd and B positions are too close together.

Exactly the same data sets as used for the kinematic refinement were used in the *MSLS* refinement resulting in a stable position for B. The determined crystal thicknesses of 37 (4), 48 (6), 99 (14) and 61 (15) Å for the zones [100], [110], [111] and [120], respectively, are too large to apply a kinematic theory successfully. In order to avoid the usual parameter dependencies, the refinement of the occupancies of the Pd and B sites were done with fixed temperature factors of 0.9 $Å^2$. Tables 6 and 7 show the resulting quantities. The occupancies refine to the values suggested by EPMA and are in agreement with the assumption made in the previous paper (Zandbergen *et al.*, 1995). Within the accuracy of our experiment, the B positions are identical to those in ThB_6.

Table 6. *The refined model of* $ThPd_xB_{6-2x}$

Space group: $Pm\bar{3}$. $a = 4.2$, $b = 4.2$, $c = 4.2$ Å, $\alpha = 90$, $\beta = 90$, $\gamma = 90°$

	x	y	z	Occupancy
Th	0	0	0	1.0
Pd	1/2	1/2	0	0.28 (2)
B	1/2	1/2	0.224 (7)	0.7 (3)

For this structure, it was essential to include an absorption factor in the calculation of the intensities. If this factor was omitted, the position of boron was directed towards the paladium position, with a resulting z coordinate of 0.12. We believe this effect is due to the existence of high areas, caused by absorption, around the other atoms in the Fourier maps.

4.3. $Ce_5Cu_{19}P_{12}$

The structure of the third example is known from single-crystal X-ray diffraction done on $La_5Cu_{19}P_{12}$ (Cava *et al.*, 1997), as shown in Table 8. In our case, the La atoms are substituted by Ce atoms.

To obtain starting coordinates, eight HREM images of the [001] direction were recorded with an increasing focus of 5 nm. The through-focus reconstruction technique (Coene, Janssen, Op De Beeck & Van Dyck, 1992)

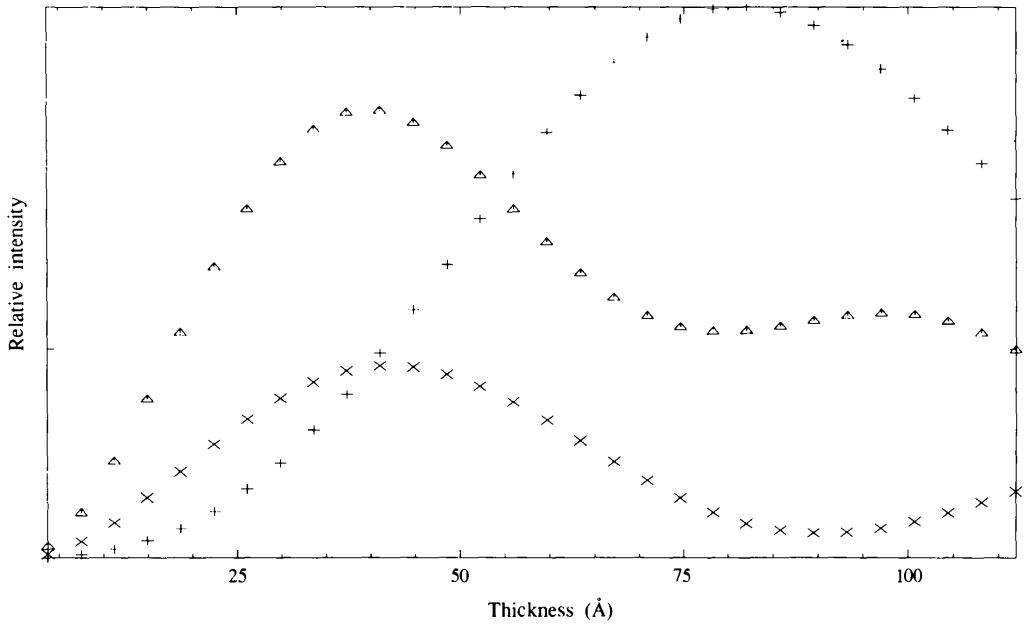

Fig. 2. Intensities as functions of thickness for $La_3Ni_2B_2N_3$: △ 200 reflection, + 002 reflection, × 103 reflection.

Table 7. *Refinement results for* $ThPd_xB_{6-2x}$

The number of reflections given are observed intensities $I > 2\sigma(I)$ which were used in the R-factor calculation.

	Overall	(100)	(110)	(111)	(120)
R (%)	3.8	2.8	0.6	9.3	2.0
Thickness (Å)		28 (7)	24 (8)	89 (16)	64 (17)
h-Laue circle		0.0	−0.2 (18)	0.1 (2)	0.2 (2)
k-Laue circle		−1.1 (14)	0.2 (18)	1.0 (4)	−0.4 (4)
l-Laue circle		−4.2 (10)	2.1 (19)	−1.0 (4)	1.4 (3)
No. of reflections	276	93	99	60	24
Absorption	0.0009 (5)				

Table 8. *The structure model of* $Ce_5Cu_{19}P_{12}$

The z coordinates were taken from the corresponding La compound. Space group: $P\bar{6}2m$. $a = 12.4$, $b = 12.4$, $c = 4.0$ Å, $\alpha = 90$, $\beta = 90$, $\gamma = 120°$

	x	y	z
Ce1	2/3	1/3	0
Ce2	x	0	1/2
Cu1	0	0	0
Cu2	x	0	1/2
Cu3	x	y	0
Cu4	x	y	1/2
Cu5	x	0	0
P1	x	0	0
P2	x	0	0
P3	x	y	1/2

Table 9. *The refined coordinates of* $Ce_5Cu_{19}P_{12}$ *compared to the coordinates of* $La_5Cu_{19}P_{12}$ *determined from single-crystal X-ray diffraction*

Coordinate	Single La	No absorption	Absorption
x_{Ce2}	0.80671	0.82 (5)	0.8112 (9)
x_{Cu2}	0.28781	0.28 (5)	0.2868 (7)
x_{Cu3}	0.37827	0.37 (5)	0.3789 (6)
y_{Cu3}	0.17247	0.18 (5)	0.1776 (7)
x_{Cu4}	0.63588	0.63 (5)	0.6354 (8)
y_{Cu4}	0.11849	0.12 (5)	0.1165 (8)
x_{Cu5}	0.45084	0.44 (5)	0.4467 (6)
x_{P1}	0.17683	0.17 (5)	0.1734 (8)
x_{P2}	0.62976	0.65 (5)	0.6457 (6)
x_{P3}	0.32167	0.63 (5)	0.3171 (4)
y_{P3}	0.84539	0.12 (5)	0.8329 (5)

was used to reconstruct the exit wave. Averaging over several unit cells and using the space-group symmetries gave the image in Fig. 3. The spots indicated in this figure were used as the starting position for *MSLS*. From the ratio of elements in the unit cell and the size of the unit cell, one can easily determine the possible positions of Ce atoms. In order to get five Ce atoms in the unit cell, one has to be located at (2/3, 1/3, 0) and the others at (x, 0, z), where $z = 0$ or 1/2. From the phase image, five peaks in the unit cell were more prominent than the others. These are the Ce atoms. For the Cu and P positions, we could not impose such an *a priori* discrimination condition.

For this crystal, several diffraction patterns in the [001] direction were measured. They varied in exposure time and crystal thickness. In the first few rounds, the P atoms were refined as being Cu atoms. By keeping the Debye–Waller factors fixed and refining the occupancies of the atoms, we were able to discriminate between these two types.† To obtain this result, it is essential to take into

† *Note added in proof*: Recent experiments show that the Ce atoms can be discriminated in the same way.

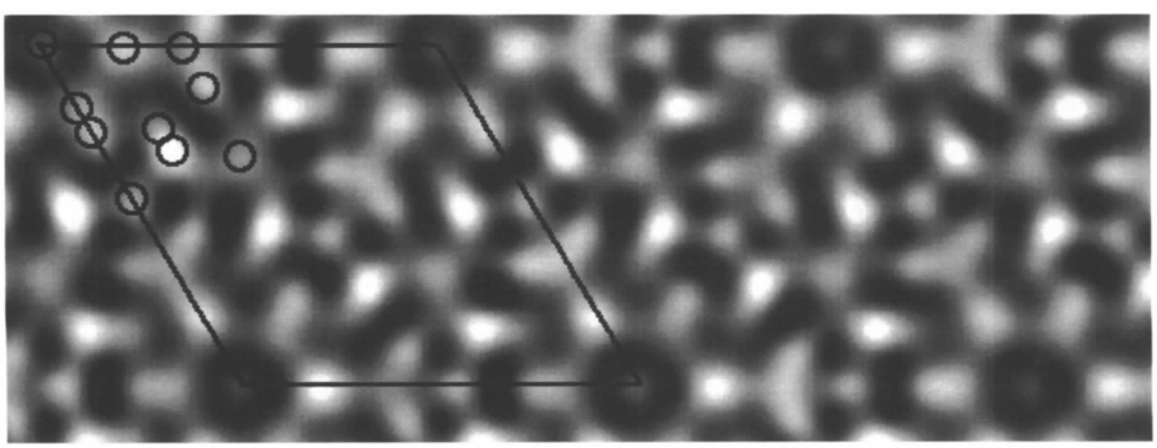

Fig. 3. Reconstructed and averaged HREM image of $Ce_5Cu_{19}P_{12}$. The indicated spots in the unit cell were taken as the starting point for the structure refinement.

Table 10. *Refinement results for $Ce_5Cu_{19}P_{12}$*

The number of reflections given are observed intensities $I > 2\sigma(I)$ which were used in the R-factor calculation.

	Overall	Set 1	Set 2	Set 3	Set 4	Set 5
R (%)	3.5	1.6	2.0	7.3	3.4	3.1
Thickness		119 (2)	125 (2)	132 (2)	171 (3)	89.3 (19)
h-Laue circle		−0.25 (6)	1.90 (8)	3.12 (9)	−0.18 (3)	3.46 (14)
k-Laue circle		−1.12 (6)	−1.16 (6)	0.51 (7)	−0.57 (4)	−1.71 (11)
l-Laue circle		0.0	0.0	0.0	0.0	0.0
No. of reflections	2476	238	154	306	137	305
Absorption	0.000476 (14)					

	Set 6	Set 7	Set 8	Set 9	Set 10
R (%)	3.5	5.5	2.2	4.7	1.6
Thickness (Å)	105.4 (17)	174 (2)	157 (3)	110 (2)	120 (2)
h-Laue circle	1.99 (8)	1.77 (5)	0.06 (4)	−0.33 (7)	−0.26 (6)
k-Laue circle	−1.02 (7)	−0.90 (4)	−0.43 (3)	−1.98 (9)	−1.11 (6)
l-Laue circle	0.0	0.0	0.0	0.0	0.0
No. of reflections	348	330	156	264	238

account several data sets from crystals of different thicknesses, since each atomic type has its own contribution to the exit wave as a function of thickness (see Fig. 4). The results of *MSLS* refinement of the structure, with the P atoms at the correct locations, using ten of these data sets are listed in Tables 9 and 10. The results, within the accuracies of the experiments, are the same as those obtained from single-crystal X-ray diffraction. Again, it was essential to refine the absorption factor. In this case, if it was omitted, the R factor indicated an error in the refinement by staying above 12% for all data sets. The coordinates of P3 especially gave problems. However, if one sets the absorption to zero and starts with the right structure, even then this position moves away from the true value.

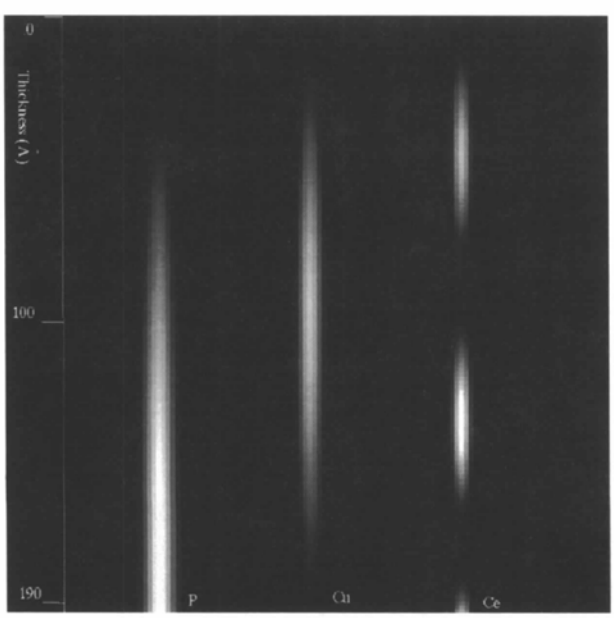

Fig. 4. The contribution of P, Cu and Ce to the exit wave as a function of thickness. The picture is a result of several multislice simulations.

The same data sets were used in a kinematical refinement, resulting in high R values (> 20%) and wrong coordinates (Zandbergen & Jansen, 1997).

5. Discussion

A least-squares crystal-structure refinement based on a multislice algorithm gives reliable atomic positions. It is superior to a procedure based on the kinematical diffraction theory, which can only be applied for thicknesses up to about 20 Å for strong scatterers. The use of the multislice algorithm expands the validity of the method to the same limits as the multislice algorithm itself; it cannot be used for crystals thicker than 150–400 Å, depending on the composition of the crystal, because above that thickness the multislice method tends to fail. The main reason for this effect is that the absorption included is only a rough approximation of the physical absorption and that inelastic scattering is neglected. *MSLS* will benefit from better scattering factors like those of Bird & King (1990). Since we are aiming to use the same crystal areas as in HREM and because crystals with such thicknesses are relatively easy to obtain, this is not a real limitation.

One has to keep in mind that, since the method is valid for crystals thinner than ~150 Å only, the determined structure may be different from the one in the bulk material. Relaxation at the surface of the crystal becomes relatively more important for these thin crystals.

Another problem may arise when the crystal area from which electron diffraction data are recorded is not of one thickness within the illuminated area, *e.g.* a wedge-shaped crystal. To test its influence, three diffraction patterns of the $ThPd_{0.65}B_{4.7}$ structure in the [100] direction were simulated. The thicknesses were respectively 35.7, 50.4 and 65.1 Å. Assuming coherency

among the different areas within the spot, the complex diffraction amplitudes, $F_{\mathbf{H}}$, were added to form a combined diffraction data set. It appeared that *MSLS* refined it to the right structure with the average thickness of 50.4 Å, even when the starting z coordinate of B was set at 0.4 Å from the real value. The same discussion as for thickness variation within the illuminated area holds for orientation variation. Both subjects are topics for further investigation.

The accuracy of the method is highly dependent on the accuracy of the atomic scattering potentials. In the examples in this paper, we used Doyle & Turner (1968) scattering factors, and the values of Smith & Burge (1959) for the missing atomic types. Among other possibilities, one can employ the X-ray potentials of Cromer & Mann (1968) using the Mott formula to transform them to electron scattering factors. One can also apply the procedure developed by Tang & Dorignac (1995) or Bird & King (1990). In order to test the effect of the type of scattering factor on our refinement procedure, we simulated diffraction patterns with both the Cromer & Mann type and the Doyle & Turner type for the $ThPd_{0.65}B_{4.7}$ structure. The correlation between these sets decreased from 0.99 for the kinematical intensities to 0.96 for intensities for a thickness of 150 Å. This correlation is so high that it is to be expected that the experimental errors will overshadow the effect of the chosen scattering power.

Since the multislice calculation that is the basis of *MSLS* is valid for perfect periodic structures only, special care has to be taken in the experimental conditions. The illuminated area of the crystal should be small in order to get a small variation in crystal thickness but not too small because too small spot sizes will cause cut-off problems since the illuminated part of the crystal is not infinite, resulting in very large overlapping spots in the diffraction pattern. This effect is used in X-ray powder diffraction to determine the particle size. In all calculations, an infinite crystal is assumed.

An amorphous layer may influence the measured integrated intensities. In principle, the background subtraction should cope with this. However, if the shape of the background at the diffraction spot cannot be predicted from the surrounding of the spot, the integrated intensity may be determined in the wrong way. If the amorphous layer contributes as a constant or as a linear function underneath a peak, it is easy to be corrected for, but failure is to be expected for more complex behaviour such as large rings around the central beam.

To avoid contamination within the microscope, the sample may be cooled. An extra advantage of cooling is that the Debye–Waller factors become smaller and that reflections with higher reflection angles can be observed. This enhances the resolution of the data.

In order to avoid radiation damage of the sample, one can use a procedure in which the area of interest is only illuminated during the actual recording of the diffraction pattern and the rest of the time the beam is at another position. With a Philips microscope, a computer-controlled beam shift to and from the area of interest makes this possible.

A small problem arises when the crystal thickness and temperature factors are refined simultaneously because these parameters are highly correlated. Raising both the thickness and the temperature factors results in almost the same least-squares sum. This is not an artefact of the calculation method but lies in the behaviour of nature. Increasing the Debye–Waller factor of an atom means a

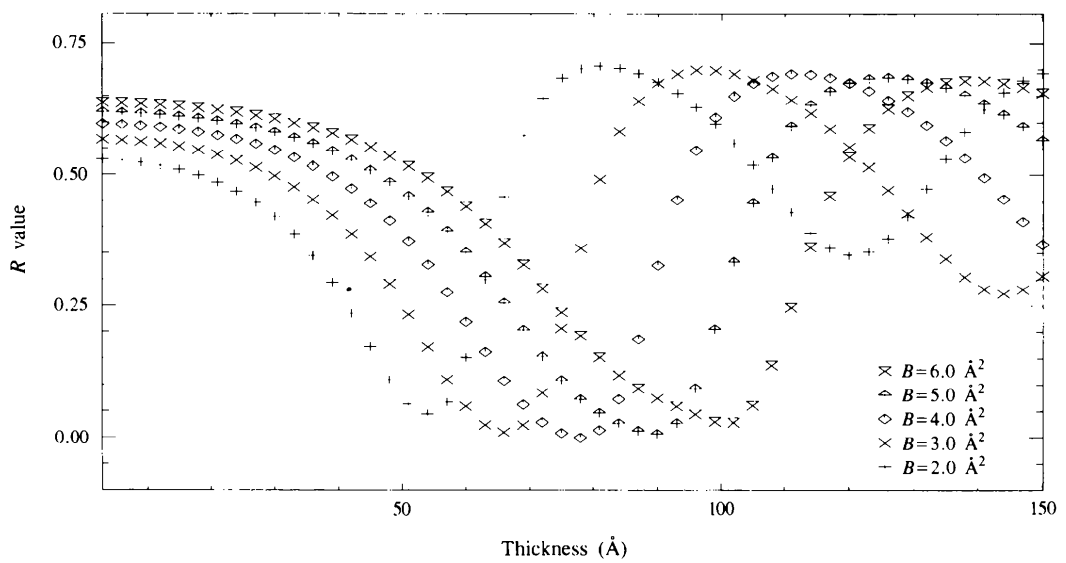

Fig. 5. The R value as function of thickness generated for a simulated diffraction pattern with several Debye–Waller factors fitted to a structure 78 Å thick with $B = 4.0$ Å^2.

less peaked scattering potential, which in turn results in a less sharply peaked interaction with the incident electron wave. Thus, in order to get the same amount of *multiple* scattering, the crystal has to be thicker. To illustrate this, diffraction patterns were generated with thickness varying from 3 to 150 Å for a crystal structure containing some La atoms positioned randomly with overall temperature factors ranging from 2.0 to 6.0 Å. To all these patterns, the same structure with thickness of 78 Å and $B = 4.0$ Å^2 was fitted using *MSLS* to get the scaling factors. Fig. 5 shows the resulting R values as a function of the thickness. $I_m^{\rm calc}$ in this case is the one with a thickness of 78 Å and B of 4.0 Å^2 and $I_m^{\rm obs}$ is the pattern with thickness and B as in the figure. All curves have a sharp minimum whose position correlates positively with the Debye–Waller factor. The actual R values of the minima are almost the same. This means that since simulated data are used here with no experimental noise, in practice one will find a rather large dependency between temperature factor and thickness. So a thickness of 50 Å and $B = 2$ Å^2 will give about the same results as a thickness of 103 Å and $B = 6$ Å^2.

The minima of the curves of Fig. 5 at larger thickness are too big to bother about. Of course, if the starting value of the thickness is too large, *MSLS* will end up in the false minimum; however, in that case the R value is far too large and one should mistrust the solution. In our experience, an R value below 8% is always near the true structure. Of course, a structure with equal atoms, as presented here, is a worst case situation.

One way to overcome the problem of the high correlation between the thickness and the temperature factors is to determine the thickness in other ways. For very thin crystals, a method to do this was reported recently (Tang, Jansen, Zandbergen & Schenk, 1995). This method is based on the fact that magnitudes of the structure factors, in kinematic approximation, should obey certain intensity statistics. Since this procedure is completely independent of the calculations used in *MSLS*, it can be used for a constrained refinement. This will be a subject for further investigation in the future. Another approach may be the use of the central beam. Since the relative intensity decreases with thickness (see Fig. 6) while the sum intensity of the diffracted beams increases, this ratio can be easily related to the crystal thickness. In principle, *MSLS* can refine the thickness if the intensity of the central beam is measured. However, the lack of dynamic range of our CCD camera prevents an accurate measurement of both the central beam and the diffracted beams at the same time.

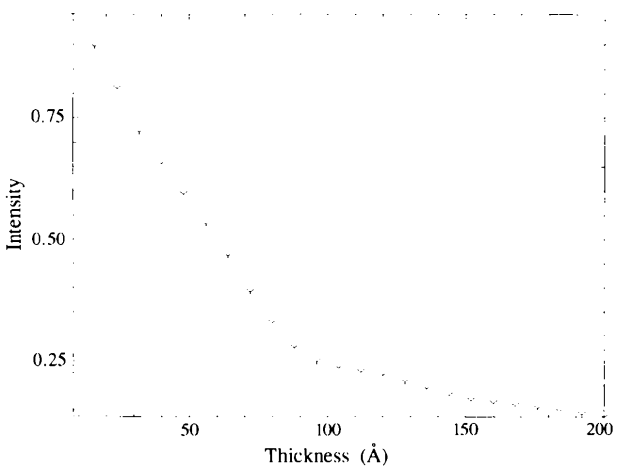

Fig. 6. Intensity of the central beam as a function of thickness for the [100] zone of $Ce_5Cu_{19}P_{12}$.

Van Dyck & Op De Beeck (1997) showed that the contribution of the atoms to the diffraction pattern depends periodically on the thickness such that at certain thicknesses columns of atoms may contribute only slightly to the diffracted beams (see Fig. 4). The periodicity of the change in scattering potential of the column depends on the atomic types and their density along the electron beam. It is obvious that including patterns with different thicknesses for the same zone direction in *MSLS* will add more information than is available for one thickness only. Especially when positions of light atoms next to heavy atoms are required, thickness series will give better information of both atomic types because they will be dominant in different diffraction patterns.

MSLS is a rather slow procedure. Typical CPU times on an IBM-RS6000 58H are 640 s for eight parameters using two different diffraction patterns of 50 and 80 Å thickness, respectively, and using 128 × 128 frames to calculate the Fourier transforms of the multislice calculation. The bottleneck is the iterative multislice algorithm. To calculate all the derivatives of formula (5), the multislice calculation has to be repeated $N + 1$ times, where N is the number of parameters to be refined. However, the method will be faster than one based on CBED as Zuo & Spence (1991) and Tsuda & Tanaka (1995) introduced. The calculation of a CBED pattern takes more time than a simple diffraction pattern of which only the integrated intensities are of interest. However, since the computers of the near future will be much faster, this is not a real problem. In principle, it should be possible to speed up the procedure by using the column approximation (Van Dyck & Op De Beeck, 1997). A disadvantage of this approach is that not all zones and not all crystals can be processed because this approach requires that the columns are not closer than 1 Å.

6. Conclusions

In the examples show here, *MSLS* proves to be a powerful tool to determine an accurate model of the crystal structure. Since the crystals needed are very small, one can investigate compounds that cannot be determined by X-rays or neutrons, *e.g.* mixtures of powders of different phases or small precipitates in a matrix. The data

collection is easy and quick: one does not have to bother about the perfect alignment of the crystal since it can be refined. This mistilt may even be used to enhance the resolution of the data. The mistilt makes it possible to observe intensities from reflections with small d spacings at one side of the diffraction pattern. Since several areas of the same compound can be refined simultaneously, *MSLS* is very powerful in determining *light* atoms next to *heavy* atoms.

The maximum thickness will be about 150 Å for compounds that contain a major fraction of strong scatterers. Fortunately, by conventional sample preparation methods, a thickness range of 50–150 Å is obtainable easily. In particular, in combination with HREM, *MSLS* is powerful. With HREM, good areas can be selected and a rough structure model can be obtained. With *MSLS*, the structure can subsequently be determined with a good accuracy.

The authors thank STW (Dutch Technology Foundation), Philips IE and the Royal Shell Research Laboratories for financing this research. Many fruitful discussions with Professor Dr D. Van Dyck and Dr M. Op De Beeck contributed to this paper. The specimens of $La_3Ni_2B_2N_3$ and $Ce_5Cu_{19}P_{12}$ were obtained from Dr R. J. Cava. The specimen of $ThPd_{0.65}B_{4.7}$ was obtained from Dr D. Z. Fisk.

References

Bird, D. M. & King, Q. A. (1990). *Acta Cryst.* A**46**, 202–208.
Cava, R. J., Siegrist, T., Carter, S. A., Krajewski, J. J., Peck, W. F. Jr & Zandbergen, H. W. (1997). *J. Solid Sate Chem.* In the press.
Coene, W., Janssen, G, Op De Beeck, M. & Van Dyck, D. (1992). *Phys. Rev. Lett.* **69**, 3743–3746.
Cowley, J. M. & Moodie, A. F. (1957). *Acta Cryst.* **10**, 609–619.
Cromer, D. T. & Mann, J. B. (1968). *Acta Cryst.* A**24**, 321–324.
Dorset, D. L., Kopp, S., Fryer, J. R. & Tivol, W. F. (1995). *Ultramicroscopy*, **57**, 59–89.
Doyle, P. A. & Turner, P. S. (1968). *Acta Cryst.* A**24**, 390–397.
Giacovazzo, C., Monaco, H. L., Viterbo, D., Scordari, F., Gilli, G., Zanotti, G. & Cati, M. (1992). *Fundamentals of Crystallography*, pp. 90–98. International Union of Crystallography/Oxford University Press.
Hovmöler, S. (1992). *Ultramicroscopy*, **41**, 121–135.
Huang, Q., Chamoumakos, B. C., Santoro, A., Cava, R. J., Krajewski, J. J. & Peck, W. F. Jr (1995). *Physica (Utrecht)*, C**244**, 101–105.
Kirkland, A. I., Saxton, W. O., Chau, K.-L., Tsuno, K. & Kawasaki, M. (1995). *Ultramicroscopy*, **57**, 355–374.
Kirkland, E. J. (1980). *Ultramicroscopy*, **15**, 151–172.
Lichte, H. (1991). *Ultramicroscopy*, **38**, 13–22.
Midgley, P. A., Saunders, M., Vincent, R. & Steeds, J. W. (1995). *Ultramicroscopy*, **59**, 1–13.
Op De Beeck, M. (1996). http://www.ruca.ua.ac.be/~modb/ROBIN/ROUND_ROBIN_main.html
Op De Beeck, M., Van Dyck, D, & Jansen, J. (1997). *Ultramicroscopy*. In the press.
Sha, B. D., Fan, H. F. & Li, F. H. (1993). *Acta Cryst.* A**49**, 877–880.
Smith, G. H. & Burge, R. E. (1959). *Acta Cryst.* **15**, 182–189.
Stadelmann, P. A. (1987). *Ultramicroscopy*, **21**, 131–146.
Tang, D. & Dorignac, D. (1995). *J. Microsc.* **179**, 191–200.
Tang, D., Jansen, J., Zandbergen, H. W. & Schenk, H. (1995). *Acta Cryst.* A**51**, 188–197.
Tsuda, K. & Tanaka, M. (1995). *Acta Cryst.* A**51**, 7–19.
Van Dyck, D. (1993). *Electron Diffraction Techniques*, Vol. 2, edited by J. M. Cowley, pp. 146–154. International Union of Crystallography/Oxford University Press.
Van Dyck, D. & Op De Beeck, M. (1992). *Proc. 12th International Congress on Electron Microscopy*, p. 26. San Francisco Press.
Van Dyck, D. & Op De Beeck, M. (1997). In preparation.
Vincent, R. & Exelby, P. R. (1995). *Acta Cryst.* A**51**, 801–809.
Zandbergen, H. W. & Jansen, J. (1997). *J. Microsc.* In the press.
Zandbergen, H. W., Jansen, J., Cava, R. J., Krajewski, J. J. & Peck, W. F. Jr (1994). *Nature (London)*, **372**, 759–761.
Zandbergen, H. W., van Zwet, J., Jansen, J., Sarrao, J. L., Maple, M. B., Fisk, Z. & Cava, R. J. (1995). *Philos. Mag. Lett.* **71**, 131–138.
Zuo, J. M., Høier, R. & Spence, J. C. H. (1989). *Acta Cryst.* A**45**, 839–851.
Zuo, J. M. & Spence, J. C. H. (1991). *Ultramicroscopy*, **35**, 185–196.